Construction and Building Materials 47 (2013) 1461–1467

Contents lists available at SciVerse ScienceDirect

Construction and Building Materials

journal homepage: www.elsevier.com/locate/conbuildmat

Utilization of circulating fluidized bed fly ash in preparing non-autoclaved aerated concrete production

Yanqing Xia *, Yun Yan, Zhihua Hu

School of Material Science and Engineering, Southwest University of Science and Technology, Mianyang 621010, China
State Key Laboratory Cultivation Base for Nonmetal Composites and Functional Materials, Mianyang 621010, China

HIGHLIGHTS

- NAAC has a substantial advantage in facilitating the manufacturing process.
- In our study, steam curing was conducted lower than 100 °C for 8–24 h after samples being cut.
- We used CFA as raw materials for making CFA non-autoclaved aerated concrete CNAAC.
- We investigated the effect of preparing parameters of CNAAC on mechanical properties.
- The optimal technological parameter for preparing NAAC in laboratory scale was obtained.

ARTICLE INFO

Article history:
Received 28 February 2013
Received in revised form 27 May 2013
Accepted 17 June 2013
Available online 17 July 2013

Keywords:
Non-autoclaved aerated concrete (NAAC)
Rheological property
Density
Strength
Microstructure

ABSTRACT

Circulating fluidized bed combustion (CFBC) fly ash (CFA) is an industrial waste from CFBC boiler of electric power plant, which is not a good supplementary cementitious material for Portland cement and concrete because its expansive feature results in unexpected deterioration of concrete in the last stage. The non-autoclaved aerated concrete (NAAC) was developed using the CFA as main raw materials in this study. To find out the effect of raw materials on the products properties, rheological property of fresh pastes, physical, chemical, mechanical and microstructure analyses were performed. The results show the reasonable dosage of CFA, cement, and lime were 65.5%, 22%, and 10%, respectively. Medium diameter of CFA particle size ranges from 9.6 μm to 23.9 μm is the most suitable for preparation of NAAC duo to the matching condition between thickening rate of the slurry and the reaction rate of aluminum powder and water. The principal minerals in NAAC are needlelike AFt and floccular C–S–H, be different from autoclaved aerated concrete (AAC).

1. Introduction

Being aware of the importance of air quality and environmental conservation, the pollution from the electric power plant by coal combustion into the atmosphere has taken serious social attention. In recent years, circulating fluidized bed combustion (CFBC) (a much more efficiently clean coal combustion technique, compared with traditional coal combustion) has caught increasing attention and is widely used all over the world, because of its effectively controlling SO_2 and NO*x* emissions [1,2]. Combusting 1t coal powder, 1/3–1/2 times limestone must be added into the fire chamber of the boiler in CFBC process, so that SO_2 generated in the process of coal-fired can be absorbed on the surface of lime powder resulting from decarbonization of limestone powder to achieve the purpose of reducing emission of sulfur dioxide and nitric oxides into atmosphere [3]. The amount of CFBC fly ash (CFA) produced by combustion of per ton of coal is 40% more than conventional pulverized coal ash. Every year, there are 120 million tons CFA stacked in China. The enormous amount of stacked CFA not only occupies land, but also pollutes water resource and soil. Therefore, it is time for developing techniques for recycling and reutilizing of CFA.

Contrary to the fly ash from conventional pulverized coal combustion boiler, CFA is not a good supplementary cementitious material for Portland cement and concrete because of the dimensional instability in the latter ages resulting from gradual hydration of CaO and $CaSO_4$ [4,5]. Some studies [6–8] demonstrate the CFA is a promising admixture for construction and building materials. Chang-seon et al. found that CFA can be effectively used in developing controlled low strength material mixture. In Prinya's study, CFA was used as a raw material for geopolymer. Takada made use of CFA as road base material.

Aerated concrete, a new wall material, has many advantages, such as lightweight, lower thermal conductivity, sound absorption and so on. Aerated concrete is usually made up of lime, cement,

* Corresponding author at: School of Material Science and Engineering, Southwest University of Science and Technology, Mianyang 621010, China.
E-mail address: 865847193@qq.com (Y. Xia).

0950-0618/$ - see front matter © 2013 Published by Elsevier Ltd.
http://dx.doi.org/10.1016/j.conbuildmat.2013.06.033

gypsum and sand (or pozzolanic materials) with traces of aluminum powder as a pore-forming agent. The aluminum reacts with lime, which releases hydrogen gas and forms a large amount of tiny bubbles distributed uniformly in the matrix [9,10]. After placed, in general, aerated concrete was cut into precise dimensional units and then cured in an autoclave where the best cure pressure is 1.0–1.2 MPa for 5–8 h [11].

Compared with the traditional autoclaved aerated concrete (AAC), non-autoclaved aerated concrete (NAAC) has a substantial advantage in facilitating the manufacturing process and reducing the cost of products. During the NAAC production, steam curing was conducted lower than 100 °C for 8–24 h after being cut. Therefore, NAAC has the feature of safety in product process with low energy consumption compared with AAC. This paper attempts to use CFA as raw materials for making CFA non-autoclaved aerated concrete (CNAAC). This work is aimed to investigate the effect of preparing parameters of CNAAC on its mechanical, physical properties and phase compositions. The optimal technological parameter for preparing NAAC in laboratory was obtained.

2. Materials and experimental program

2.1. Materials

CNAAC mixture slurry were prepared with P.O42.5R, CFA, lime, phosphogypsum (PG), blast furnace slag and water. CFA (Baima electric power plant, Neijiang, Sicuan Province, China) was grinded finely with medium diameters of 6.1 μm, 9.6 μm, 15.5 μm and 23.9 μm, respectively. In this study, Lafarge P.O 42.5R cement was used. PG contains 15.99% crystal water and 0.18% soluble phosphorus element. Aluminum powder was also used in fresh aerated concrete mixture as a gas generating agent. Lime was supplied from Jiangyou, Sicuan Province, China, whose digestion time was 3.4 min resulting from containing 84.2% active ingredient CaO. The chemical composition of the principal raw materials was given in Table 1.

2.2. Preparation of specimens

In the study, all of the CNAAC specimens were molded by following steps: 1 kg dry ingredients were mixed in a laboratory mixer for 1 min, according to mix proportions (Table 2), then 85% water in which 5 g Na_2SO_4 and 0.45 g TEA had been dissolved was added to the mixture and it is quickly mixed for 1 min. And then poured the remaining water dispersing 1.1 g aluminum powders into the mixer and the mixture is quickly mixed again for 30 s. At last, the slurry was molded in 70.7 mm × 70.7 mm × 70.7 mm molds. After being molded, for samples X1–X20, the specimens undertook the two steps curing cycles. At the first step, specimens were heated in the steam curing box at 50 °C for 4 h, and then 60°Csteam curing was conducted for 24 h after being cut into predetermined dimension. Specially, for X0, there were three different curing method after being cut: (1) the specimens were cured in the 90% R.H. chamber at 20 ± 1 °C (standard curing); (2) the specimens were cured at 60 °C for 24 h before standard curing and (3) The specimens were cured at 90 °C for 24 h before standard curing.

2.3. Rheological property test

In order to investigate into the influence of the particle size and the dosage of raw materials on the rheological property of CNAAC paste, a rotary viscometer (Viskomat NT, Schlebinger, Germany) which consists of internal and external steel cylinder, paddle blades and data processing system was used to measure critical yield stress and plastic viscosity of slurry. Plotting torque (T) against speed of rotation (s) determined the rheological parameters and curve of fresh CNAAC paste according to the Bingham's model expressed as

$$T = T_0 + hs \quad (1)$$

where T_0 (N mm) and h (N mm min) are directly related with critical yield stress and plastic viscosity, respectively. A series of samples were prepared in accordance with 2.2 and their composition is listed in Table 2, the water solid ratio is 0.58. The slurry of CNAAC was placed in the internal steel cylinder. During the measurement, the temperature of paste was kept 35 ± 1 °C by a temperature controller. Applied speed of rotation of each sample was ranged from 0 to 180 rpm and the speed increased by 15 rpm every 30 s.

2.4. Characterization techniques

XRF offered chemical analyses of the raw materials. Mineralogical analysis of CFA was conducted by using an X-ray diffractometer which was carried out on a D/max-IIIA diffractometer (Rint2200 with a nickel filtered Cu Kα). Particle size distribution of CFA was analyzed by Mastersizer 2000 (Malvern, England). TAM AIR08 (TA, USA) was used in testing the hydration heat of CFA. Water requirement of normal consistency and setting time of CFA were determined according to Chinese standard GB/T1346-2001. Compressive strength of CFA was done by using 40 mm × 40 mm × 160 mm prism specimen with sand to CFA ratio of 3.0 and water to CFA ration of 0.5 according to Chinese standard GB17671-1999. Three dried cube specimens of 70.7 edge length were used for measuring compressive strength. Three other cube specimens were dried in a ventilated oven at 60 °C for not less than 48 h, and until two successive determination of mass at intervals of 2 h show an increment of loss not greater than 0.2% of the last previously determined mass of the specimen. For the mineralogical investigation, the CNAAC was dried at 60 °C and ground, then XRD analyses were conducted. The microstructure of specimens was observed by using EVO 18 scanning electron microscopy (Zeiss, Germany).

3. Results and discussion

3.1. Mineralogical and microstructural analyses

The mineralogical compositions of CFA shown in Fig. 1 are quartz (SiO_2), anhydrite ($CaSO_4$II), hematite (Fe_2O_3) and $Ca(OH)_2$. The dissolution and crystallization of $CaSO_4$II results in expansion of solidified CFA pastes. The presence of $Ca(OH)_2$ attributes to the reaction of f-CaO with water vapor in the air during the CFA storage. As shown in Fig. 2, the CFA consists of irregular and porous particles, which can lead to a high water requirement. There are two reasons for the loose microstructure of the particles. The first is the combustion temperature. A low temperature, 850–900 °C is

Table 1
The chemical composition of the main raw materials.

Composition (%)	SiO_2	Al_2O_3	Fe_2O_3	CaO	TiO_2	R_2O	SO_3	f-CaO	P_2O_5	Loss
CFA	36.69	14.32	11.91	19.49	1.21	1.15	13.69	4.65	–	5.80
Cement	19.66	5.00	3.45	64.11	0.85	0.66	4.31	0.70	–	3.60
PG	14.50	0.74	0.12	26.79	–	–	37.25	–	5.06	15.99
Slag	31.40	12.53	4.56	39.87	1.93	1.47	1.62	–	–	4.63

Table 2
The mixture proportion of CNAAC.

Specimen type	Median particle size of CFA (μm)	CFA (wt%)	Cement (wt%)	Lime (wt%)	PG (wt%)	Slag (wt%)	Water to solid ratio (W/S)
X0 (Reference)	15.5	65.5	20	10	1.5	3	0.58
X1 (2,3,4)	15.5	69.5 (67.5, 63.5, 61.5)	16 (18, 22, 24)	10	1.5	3	0.58
X5 (6,7)	15.5	70.5 (60.5, 55.5)	20	5 (15, 20)	1.5	3	0.58
X (9, 10,11)	23.9	65.5	20	10	1.5	3	0.56 (0.58, 0.60, 0.62)
X12 (13,14,15)	9.6	65.5	20	10	1.5	3	0.56 (0.58, 0.60, 0.62)
X16 (17,18,20)	6.1	65.5	20	10	1.5	3	0.56 (0.58, 0.60, 0.62)

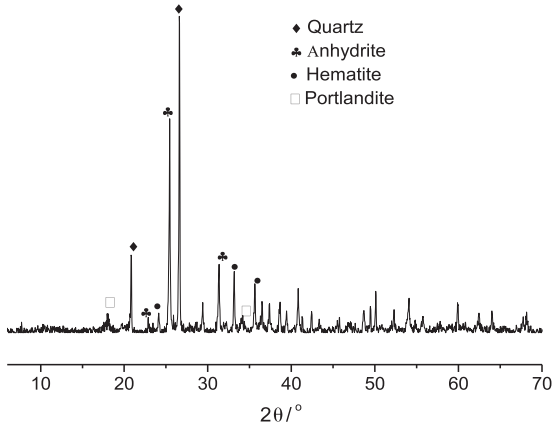

Fig. 1. XRD patterns of CFA.

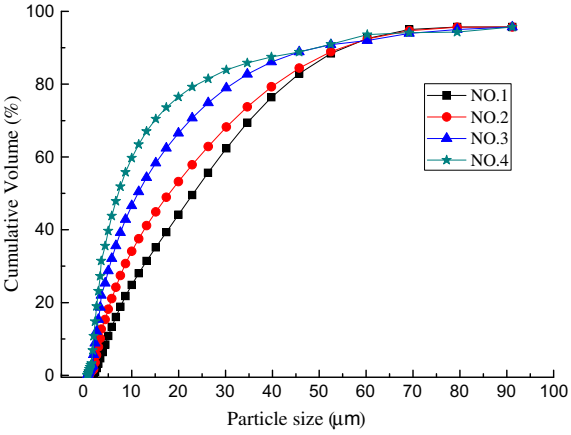

Fig. 3. Cumulative particle size distribution of CFA.

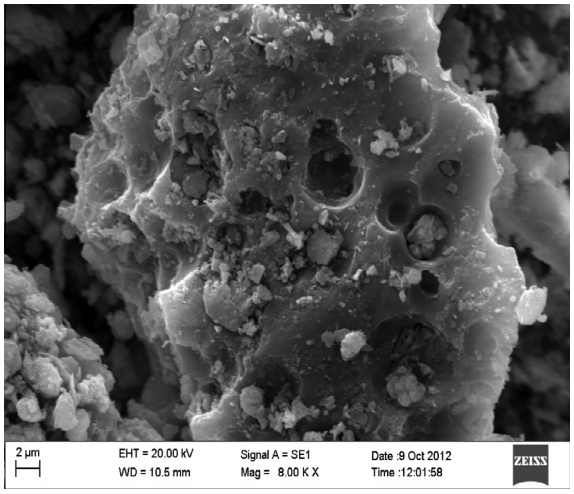

Fig. 2. SEM analysis of CFA.

not high enough to melt clay minerals and the reactions should have remained in the solid state [12]. The second is CO_2 emission which is generated from coal combustion and limestone decomposition. Coarse CFA exhibits low pozzolanic activity owing to the agglomeration f-CaO, so mechanical grinding is used to produce finely ground particles, make the f-CaO distributing homogeneously and improve the self-cementitious properties.

3.2. Particle distributions of CFA

CFA powder samples with four different medium diameters were prepared by grinding the original CFA (No. 1), as indicated in Table 3. The cumulative particle size distribution (PSDs) for all CFA samples (No. 1, No. 2, No. 3, and No. 4) are plotted as a function of particle diameter in Fig. 3. The result shows that PSDs of the four samples differs in the fraction of lesser than 60 μm. With increasing grinding time, the whole size distribution is shifted towards smaller diameters and the median particle size (MPs) decreases from 23.9 μm to 6.1 μm.

Exothermal behavior of CFA water system was shown in Fig. 4. According to Fig. 4, it was observed that CFA with water was an exothermic reaction, and without an external force, it reacted spontaneously. The result implies that CFA is self-cementitious. It can be also seen from Fig. 4 that the better fineness CFA hydrates more rapidly, leading to a higher hydration heat. For example, No. 1 generated 65 J/g of hydration heat in 7 days. However, No. 3 and No. 4 were 100 J/g and 145 J/g, respectively. This indicates that the finer CFA is, the faster the reaction rate between CFA and water. Hence, the fineness of CFA utilized in NAAC should have a dominant effect on either fresh paste or mechanical performances of NAAC.

Setting time and self-cementitious compressive strength of CFA is shown in Table 3. The trend shows a decrease in initial and final setting time with decrease of CFA fineness from 23.9 μm to 6.1 μm due to the speedy dissolution reaction of f-CaO, $CaSO_4$ and active silica/active alumina. The self-cementitious strength of CFA increases with the decrease of MPS values of CFA. If the MPS value is over 10 μm, it has a little of effect on self-cementitious strength of CFA, while it increases greatly when the value is below 10 μm. For example, when the MPS value is 6.1 μm, the compressive strength at 7 days and 28 days are 13.5 MPa and 18.7 MPa respectively, which are 5.4 and 1.5 times as great as that of No. 1. The decrease of MPS value is beneficial to the dissolution of active silica/ alumina in the CFA, and the hydration of $CaSO_4$II and f-CaO, which accelerate the generation of ettringite (AFt), C–S–H and $CaSO_4{\cdot}2H_2O$.

Water requirement of CFA at normal consistency is higher than that of cement (26.5%), which may be due to water absorption of higher f-CaO and anhydrite content [13,14] and looser microstructure of CFA. Water requirement of normal consistency decreases with the decrease of CFA medium diameter, which ascribes to better grain size distribution and decentralize of CFA.

Table 3
Self-cementitious properties of CFA.

CFA	Median particle Size (MPS) (μm)	Water requirement of normal consistency (%)	Setting time (min)		Compressive strength (MPa)	
			Initial	Final	7 d	28 d
No. 1	23.9	43.4	1136	1383	2.5	12.2
No. 2	15.5	38.3	451	507	5.6	13.9
No. 3	9.6	36.6	235	272	8.4	15.8
No. 4	6.1	35.8	64	90	13.5	18.7

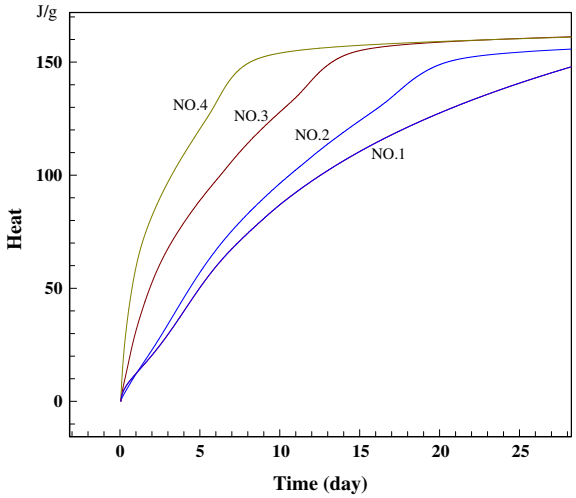

Fig. 4. Cumulative heat release for hydration under isothermal conditions for w/c = 0.8 model CFA pastes.

3.3. Rheological property

As previously mentioned, aluminum powder is mixed into the mortar resulting in a mass of increased slurry volume scheduled to entrapped H_2-gas generating from the reaction between Al and calcium hydroxide, and then a porous structure conserved in hardening stage. The tiny bubbles size and quantity of artificial air pores are enslaved to the rheological properties of the pastes. Every bubble's size and stability not only connect with bubble internal and external pressure but also relate to the paste viscosity.

Flow curves of the studied CNAAC suspensions have been shown in Figs. 5 and 7. The relative viscosity (h) and relative yield stress (T_0) are determined from these flow curves as shown in Table 4, according to the Bingham's model expressed as Eq. (1).

The influence of cement dosage on the rheological properties of CNAAC pastes as shown in Fig. 5 and Table 4. The results show that the relative yield stress (T_0) of CNAAC pastes slightly decreases with the cement dosage, while the effect of the dosage on h value is significantly less pronounced. The water requirement of CFA (Table 4) is higher than that of cement (27%), thus, the greater the amount of CFA replacement with cement, the greater is the reduction of yield stress.

Fig. 6 and Table 4 illustrate the rheological properties of fresh CNAAC pastes with the increase of the lime quantity added (samples X_0, X_5–X_7). The results show that the relative yield stress and viscosity of samples tend to be considerably increased with the increase of the lime quantity added. For example, the relative

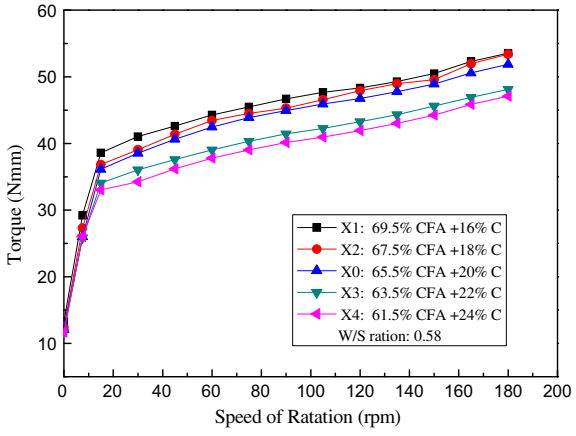

Fig. 5. Influence of cement dosage on rheological properties of CNAAC pastes.

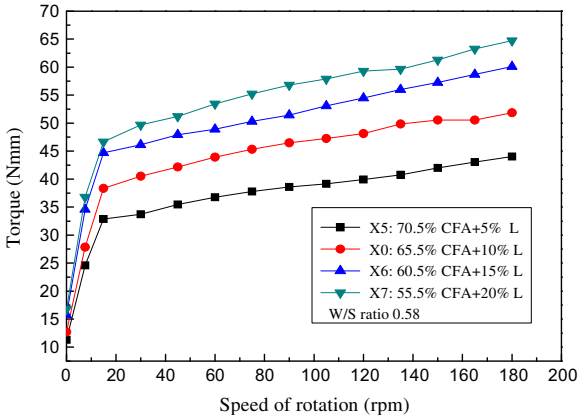

Fig. 6. Effect of lime dosage on rheological properties of CNAAC pastes.

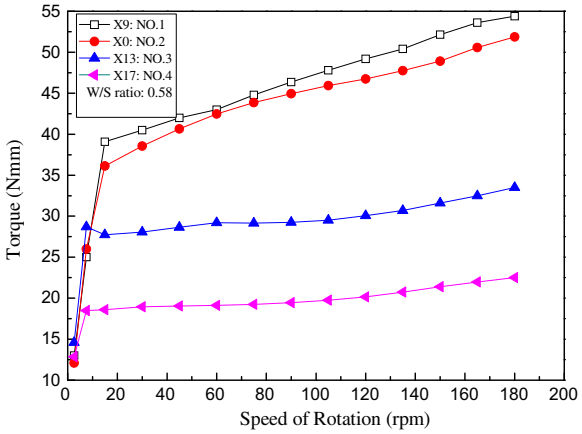

Fig. 7. Influence of CFA fineness on rheological properties of CNAAC pastes.

yield stress is 32.32 N mm when lime quantity is at 5% (X5) and that is increased to 36.21 N mm at 10% (X0) and to 46.75 N mm at 20% (X7), respectively, which indicates that lime can dramatically increase the relative yield stress of CNAAC paste. Lime can instantly react with water to slake lime and then dissolve in water to oversaturation. The newly created slaked lime is irreversible $Ca(OH)_2$ micelles which carry a positive charge because of its preferential adsorption of Ca^{2+} from the solution. In the other hand, when the CFA particle is mingled with water, Si and Al atoms on the particle surface hydroxylate owing to adsorption of OH^- which carries negative charges [14]. For the oppositive electrical property of $Ca(OH)_2$ micelles and CFA particle results in the agglomeration of particles and then the setting of CNAAC paste. Therefore, adding lime in CNAAC can increase the relative yield stress (T_0) and the relative viscosity (h) of pastes.

Fig. 7 demonstrates the torque (T) of the samples (X9, X0, X13, X17) with different CFA particle size as a function of speed of rotation (s). It can be observed that the samples with finer CFA (X0, X13 and X17) show relatively low yield stress and high flow behavior index when compared to the sample X9, being easier to flow. Among these samples, the relative viscosity (h) is 0.97 N mm min when the MPS value is 23.9 μm and that is decreased to 0.22 when MPS value is 6.1 μm.

3.4. Bulk density and compressive strength

3.4.1. Effect of cement

As can be observed in Fig. 8, the compressive strength results indicate that the dosage of cement at a certain percentage is able

Table 4
The effect of UA quantity and fineness on the rheological properties of CNAAC paste.

Sample	CFA-cement						CFA-lime				MPS of CFA		
	X1	X2	X0	X3	X4	X5	X0	X6	X7	X9	X0	X13	X17
$h \times 0.1$ (N mm min)	0.83	0.92	0.87	0.79	0.82	0.65	0.87	0.93	1.00	0.97	0.87	0.32	0.22
T_0 (N mm)	38.62	36.79	36.21	33.88	32.33	32.32	36.21	43.35	46.75	37.62	36.21	26.78	17.86
Correlation coefficient	0.97	0.96	0.96	0.98	0.98	0.98	0.98	0.99	0.96	0.99	0.96	0.92	0.99

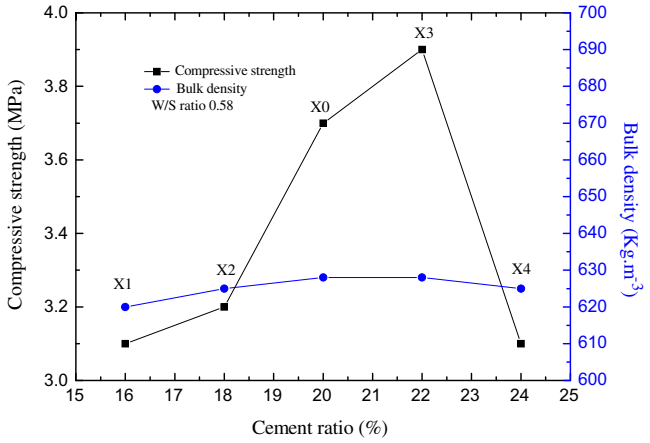

Fig. 8. Effect of cement on compressive strength and bulk density of CNAAC.

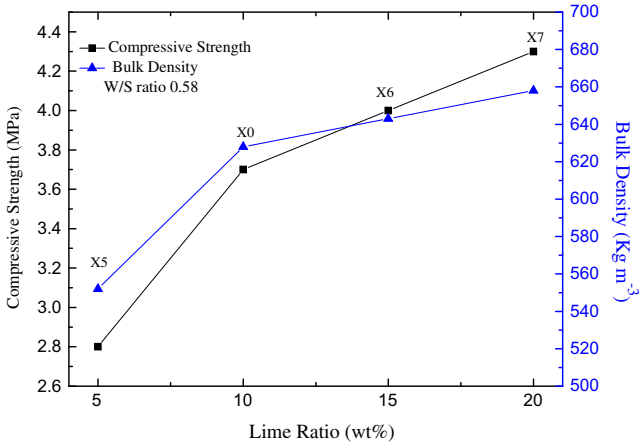

Fig. 9. Influence of lime on compressive strength and bulk density of CNAAC.

to enhance the strength of CNAAC. It has been observed that the dosage of cement up to 22% leads to the maximum strength and gradual reductions in strength are observed beyond the dosage of 22% cement. It is interesting to note that the cement content which ranges from 16% to 24% affects bulk density slightly.

Increasing quantities of cement contribute to pastes stiffness rate and accelerates the strength development; furthermore, the formation rate of tiny bubbles increases with the dosage of cement due to the pH of pastes increasing [15]. It is very important to ensure the dosage of cement in the mixture because the balance between stiffness rate of slurry and the formation rate of tiny bubbles can be maintained under this condition.

3.4.2. Effect of lime

The results of compressive strength and density with respect to lime ratio are displayed in Fig. 9. This figure clearly indicates that the increase of lime content in the mixture increases both strength and density of CNAAC. As described in Section 3.3, excessive lime leads to the significant increase in relative yield stress and viscosity of fresh pastes making the specimen not only heavier but also higher compressive strength resulting from the dense structure, because the stiffness rate of pastes is faster than the formation rate of miniature bubbles resulting into incomplete expansion of the mixture.

3.4.3. Effect of fineness

The bulk density and compressive strength test results of CNAAC specimens versus MPS value of CFA are graphically presented in Figs. 10 and 11, respectively. These show that the particle size of CFA used as the raw material influenced the mechanical properties of CNAAC as following: the coarser is the CFA, the lower are the bulk density and compressive strength. The fineness of CFA undoubtedly influences the working process of aluminum powder that determines the mix expansion of fresh pastes ultimately controlling CNAAC density and strength. Among these samples, the bulk density and strengths of the CNAAC increase by 30% and 47% with the decreasing of the MPS value from 23.9 μm to 6.1 μm when the W/S ratio is 0.58. This finding seems to be inconsistent with rheological property of fresh pastes containing finer CFA. In fact, although the fresh pastes containing finer CFA have high flow index behavior and low yield stress (Fig. 7), finer CFA requires less time to achieve set (Table 3) under the same W/S ratio, so that the setting time of pastes is faster than the formation rate of tiny bubble resulting in the creation of a lesser pores entrapped within the hardened mixture. Thus, appropriate particle size of CFA is advantageous to the working process of aluminum powder.

3.4.4. Effect of initial temperature

Under the condition of pre-defined mix proportion (X0), the pouring temperature is an important factor affecting the performances of the products due to its disturbing balance between the stiffness rate of CNAAC paste and the rate of hydrogen gas-generating. As shown in Fig. 12, when the pastes initial temperature is lower than 31°Cor higher than 39 °C, the unit weight of specimens is more than 630 kg/m^3. As a consequence, the pouring temperature

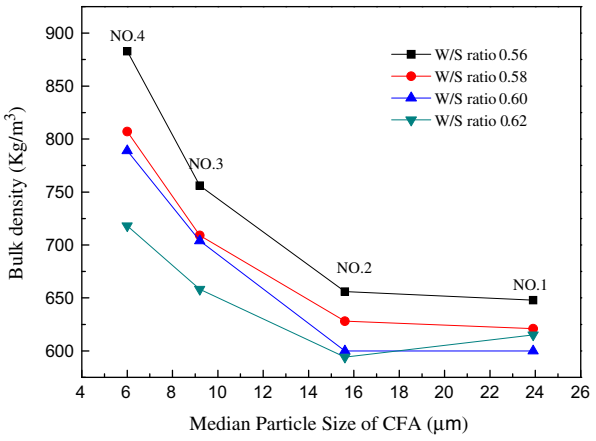

Fig. 10. Effect of CFA fineness on bulk density.

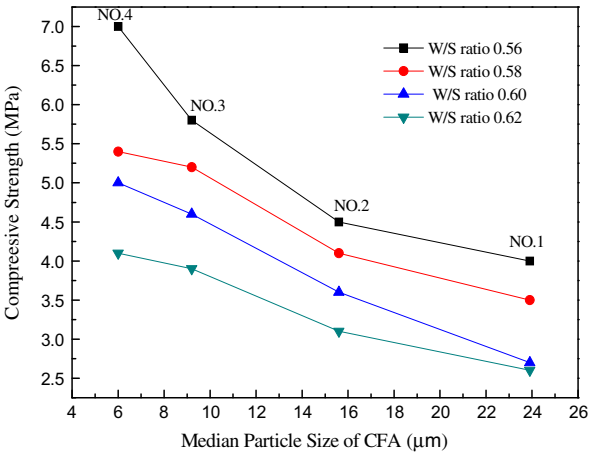

Fig. 11. Influence of CFA fineness on compressive strength.

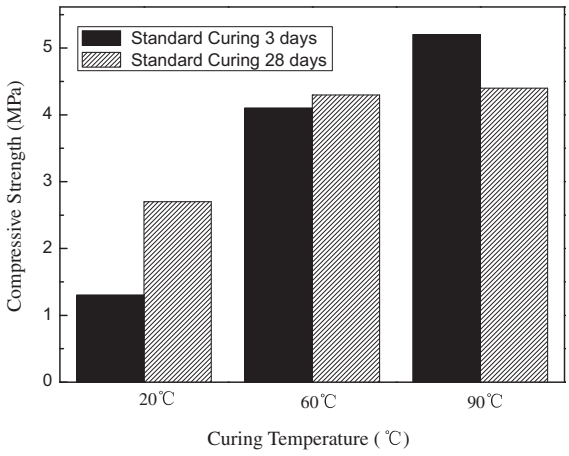

Fig. 13. Influence of curing temperature on compressive strength.

between 31 °C and 39 °C is good for bodying speed of the paste in harmony with the formation of tiny bubbles. The aluminum powder reacts with lime slowly in low temperature paste; In contrast, with the temperature increasing, stiffness rate and the formation rate of tiny bubbles are accelerated, what is more, the temperature impact stiffness rate greatly.

3.4.5. Effect of curing temperature

As can be observed in Fig. 13, the strength of X0 is furthermore affected by the curing temperature. The higher the curing temperature, the greater the compressive strength at 3 days. There is a variation in strength value of specimens with different curing temperature when the standard curing process is prolonged from 3 days to 28 days. Strengths of X0 (20 °C) and X0 (60 °C) increase by 107.7% and 4.9%, respectively, while the strength of X0 (90 °C) reduces by 15.4%. The higher increment in the strength of X0 (20 °C) occurs due to the densification of its microstructure when C–S–H gel is formed. However, the decrease in strength of X0 (90 °C) is believed to be a result of a less uniform distribution of hydration products in the pastes due to the initial rapid hydration [16].

3.5. Microstructural and mineralogical analyses of CNAAC

The XRD patterns of X0 samples under different curing temperature and age are shown in Fig. 14. As indicated in Fig. 14, the CNAAC contain AFt and calcite besides unreacted quartz, anhydrite and hematite. The ettringite (AFt) diffraction peaks appeared in all samples, and the intensity increased with increasing age and curing temperature. AFt which comes from cement hydration and the reaction of $Ca(OH)_2$, anhydrite, and active alumina dissolved from CFA is in favour of hardening and strength development of CNAAC paste. Comparing spectra of samples (20 °C, 60 °C and 90 °C), the peaks of quartz decreased significantly, indicating high curing temperature can promote the pozzolanic reaction. In addition, feeble $Ca(OH)_2$ can be found in samples for hydration of C_3S and lime slaking.

Micrographs of X0 at different curing temperature and age are shown in Fig. 15. Fig. 15 presents that higher curing temperature is favorable for the densification of microstructure at the early age. CNAAC with standard curing (Fig. 15a) shows tiny AFt crystals and amorphous C–S–H gels, a completely different structure as compared to that of the 90 °C moist-cured sample (Fig. 15c). AFt formed at standard curing are about 1–2 μm long and 0.1–0.2 μm wide, while formed in 60 °C and 90 °C are 2–4 μm long and 0.5–1 μm wide. In addition, C–S–H gels formed at standard curing are amorphous, while formed in 60 °C and 90 °C are fibrous. At the age of 28 days, for standard cured and 60 °Cmoist-cured samples (Fig. 15a and b), AFt crystals grow mixed with C–S–H and the denser microstructure is formed, but 90 °C moist-cured sample (Fig. 15c) presents loose microstructure. Therefore,

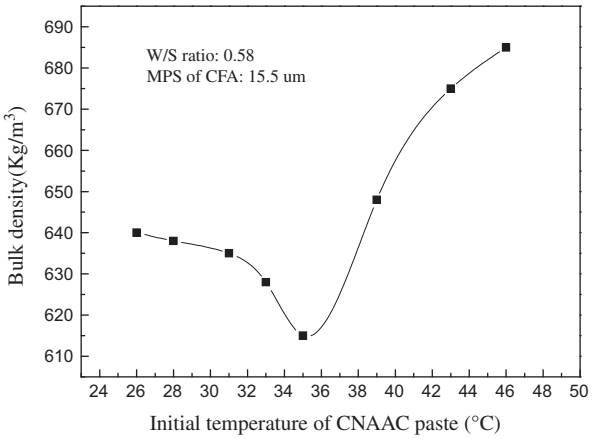

Fig. 12. Effect of initial temperature on bulk density.

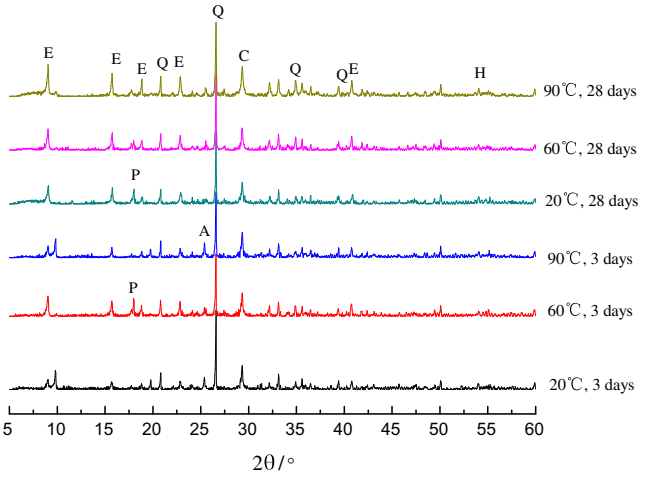

Fig. 14. XRD patterns of hydrated X0 (Q-quartz, E-ettringite, C-calcite, A-anhydrite, H-hematite, P-portlandite).

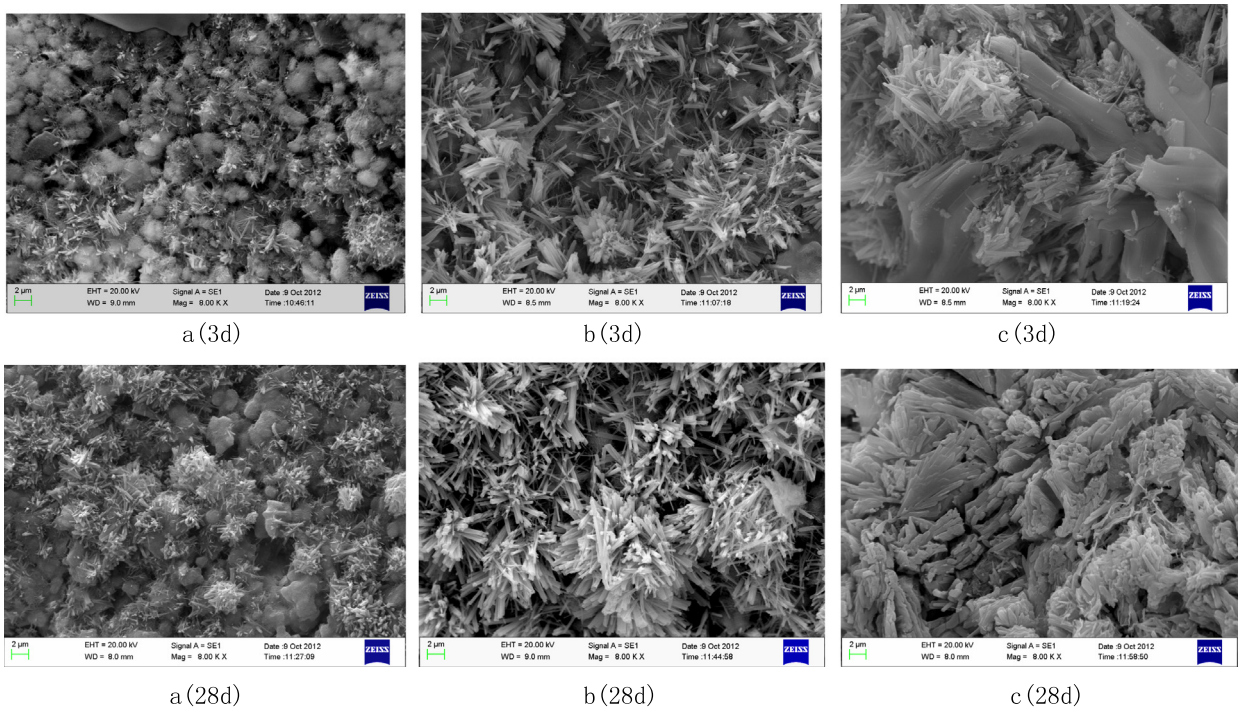

Fig. 15. Micrographs of X0. (a) standard curing, (b) 60 °C steam curing for 24 h before standard curing and (c) 90 °C steam curing for 24 h before standard curing.

compact degree of CNAAC pore wall is closely related to curing temperature and age.

4. Conclusions

This study has shown that the CFA can be used as raw materials in CNAAC production. On the basis of test results, the following conclusions should be drawn:

(1) CFA can set and harden after adding water. The finer CFA can be beneficial to decrease the relative yield stress and viscosity of fresh pastes, but interestingly, the bulk density and compressive strength of NAAC increase with the fineness owing to the setting time of pastes is faster than the formation rate of tiny bubble. As seen from test results, the MPS value of CFA ranges from 9.6 μm to 23.9 μm is conducive to the working process of aluminum powder.
(2) Cement and lime in CNAAC both can influence rheological property of pastes. The greater the amount of cement, the greater is the reduction of relative yield stress. However, the relative yield stress and viscosity tend to be increased with the increase of the lime quantity added.
(3) According to physical and mechanical tests, an optimal proportion of CNAAC was determined to be 63.5%–65.5% for CFA, 20%–22% for cement, 10% for lime, 1.5% for PG and 3% for slag.
(4) That initial pouring temperature of fresh pastes ranges from 31 °C to 39 °C is good for stiffness rate of the pastes in harmony with hydrogen gas-generating.
(5) The main minerals in CNAAC are needlelike AFt and floccular C–S–H besides quartz and other residual mineral from the CFA.

Acknowledgments

The authors want to acknowledge the financial support of the National Science and Technology support programs (2011BAA04B04 and 2011BAE14B05) of China, the Open Project of State Key Laboratory Cultivation Base for Nonmetal Composites and Functional Materials (11zxfk26) and thank the administrators of the fund of their support in our research.

References

[1] Sheng Dang, Hong wei Wang, Huang Hong, et al. Properties of CFBC fly ash & slag and its application. Int Electr Power China 2004;8:55–8.
[2] Anthony EJ, Granatstein DL. Sulfation phenomena in fluidized bed combustion systems. Prog Energy Combust 2001;27:215–36.
[3] Hong wei Zheng, Wang Hong. General utilization of CFBC fly ash. Fly Ash Utilization 2000;4:53–6.
[4] Xiang Guo Li, Quan-bin Chen, Huang uai Zhong, et al. Cementitious properties and hydration mechanism of circulating fluidized bed combustion (CFBC) desulfurization ashes. Constr Build Master 2012;36:182–7.
[5] Sheng Guang hong, Zhai Jianping Zhai, Li Qin, et al. Utilization of fly ash coming from a CFBC boiler co-firing coal and petroleum coke in Portland cement. Fuel 2007;86:2625–31.
[6] Shon Chang-seon, Saylak Don, Zollinger Dan G. Potential use of stockpiled circulating fluidized bed combustion ashes in manufacturing compressed earth bricks. Constr Build Master 2009;23:2062–71.
[7] Chindaprasirt Prinya, Rattanasak Ubolluk. Utilization of blended fluidized bed combustion (FBC) ash and pulverized coal combustion (PCC) fly ash in geopolymer. Waste Manage 2010;30:667–72.
[8] Takada T, Hashimoto I, Tsutrisumi K. Utilization of coal ash from fluidized bed combustion boilers as road base materials. Resour Conser Recycl 1995;14(2):69–77.
[9] Mostafa NY. Influence of air-cooled slag on physicochemical properties of autoclaved aerated concrete. Cem Concr Res 2005;35:1349–57.
[10] Karakurt Cenk, Kurama Haldun, Topcu Ilker Bekir. Utilization of natural zeolite in aerated concrete production. Cem Concr Compos 2010;32:1–8.
[11] Z WU Z. The development and application of building materials with fly ash. Beijing: Chinese Buiding Materials Industry Press; 2002.
[12] Jue shi Qian, Hong wei Zheng, Yuan ming Song. Special properties of fly ash and slag of fluidized bed coal combustion. J Chin Ceram Soc 2008;36(10):1396–400.
[13] Zhi Wang. Study on properties and utilization in building materials of bottom ashes from circulating fluidized bed combustion. PhD. dissertation. Chongqing: Chongqing University; 2002 [in Chinese].
[14] Guanghong Sheng, Qin Li, Jian ping Zhai. Investigation on the hydration of CFBC fly ash. Fuel 2012;98:61–6.
[15] Zhang JN, Gu TZ. Aerated concrete production process. WuHan: Wuhan University of Technology Press; 1992.
[16] Türkel Selcuk, Volkun, Alabas. The effect of excessive steam curing on portland composite cement concrete. Cem Concr Res 2005;35:405–11.